Food and Chemical Toxicology 132 (2019) 110676

Contents lists available at ScienceDirect

Food and Chemical Toxicology

journal homepage: www.elsevier.com/locate/foodchemtox

Oleanolic acid attenuates cisplatin-induced nephrotoxicity in mice and chemosensitizes human cervical cancer cells to cisplatin cytotoxicity

Iva Potočnjak, Lidija Šimić, Iva Vukelić, Robert Domitrović*

Department of Medical Chemistry, Biochemistry and Clinical Chemistry, Faculty of Medicine, University of Rijeka, Rijeka, Croatia

ARTICLE INFO

Keywords:
Oleanolic acid
Cisplatin
Kidney
Cervical cancer cells
Apoptosis
Autophagy

ABSTRACT

Oleanolic acid (OA) is a natural triterpenoid that possesses numerous beneficial health effects such as antioxidant, anti-inflammatory and anti-apoptotic activities. In this study, we investigated the therapeutic effect of OA (10 and 40 mg/kg) on cisplatin (CP)-induced (13 mg/kg) nephrotoxicity. Treatment with OA 40 mg/kg once daily for 2 days, 48 h after CP-intoxication, ameliorated the increased serum markers and histological features of kidney injury. CP administration increased renal expression of antioxidant and anti-inflammatory markers, which was reduced by OA. The increase in proapoptotic caspase-3 and -9 activations, with concomitant increase in poly (ADP-ribose) polymerase (PARP) cleavage, were dose-dependently inhibited by OA. Treatment with OA also ameliorated microtubule-associated protein 1A/1B-light chain 3B (LC3B)-II and autophagy-related protein (Atg) 5 expression induced by CP. The suppression of CP-induced oxidative stress, apoptosis, autophagy and inflammatory response by OA coincided with the inhibition of extracellular-regulated kinase (ERK) 1/2, signal transducer and activator of transcription (STAT) 3 and nuclear factor-kappa B (NF-κB). Interestingly, OA increased CP cytotoxicity in HeLa cervical cancer cells by inducing cytotoxic autophagy. The chemosensitization of HeLa cells to CP suggests a potential beneficial effect of OA in cervical cancer patients due to reduced CP dosage requirements, which requires further investigation.

1. Introduction

Cisplatin (CP) is a chemotherapeutic agent used for the treatment of various cancers (head and neck, lung, testis, ovary and breast) (Perse and Veceric-Haler, 2018). The anticancer action of CP is mediated by the formation of deoxyribonucleic acid (DNA) intra-strand or inter-strand crosslinks (Dasari and Tchounwou, 2014). CP binds to purine residues thus causing DNA damage in cancer cells, blocking cell division and resulting in apoptotic cell death. Oxidative stress is one of the most important mechanisms involved in CP cancer cell cytotoxicity, with the mitochondria as the primary target for CP-induced oxidative stress (Marullo et al., 2013).

Treatment with CP has several adverse side effects such as nephrotoxicity, hepatotoxicity, cardiotoxicity and ototoxicity and it is associated with drug resistance (Dasari and Tchounwou, 2014). Kidneys are the major route for CP excretion and they accumulate CP to a greater degree than other organs. Active accumulation of the drug by renal parenchymal cells results in cell injury and death. The most serious adverse effect of CP therapy is acute kidney injury (AKI), which occurs in 20–30% of patients. The CP-induced nephrotoxicity is widely used as an experimental model of AKI (Ozkok and Edelstein, 2014).

Both experimental and clinical data show that oxidative stress plays a pivotal role in CP-induced renal damage (Oun et al., 2018). Oxidative stress, caused by the overproduction of reactive oxygen species (ROS), has been implicated in the pathophysiology of CP nephrotoxicity through various mechanisms (Al-Kahtani et al., 2014). CP-induced ROS production that overcomes endogenous antioxidative defense leads to inflammation and boosts mitochondrial damage, resulting in apoptotic cell death. It was shown that antioxidant agents present a potential approach for ROS scavenging and attenuation of CP-induced nephrotoxicity (Gomez-Sierra et al., 2018). Plant-based products play an essential role in healthcare, both as pharmaceutical agents and a source of bioactive molecules (Cragg and Newman, 2013; Domitrovic and Potocnjak, 2016). Phytochemicals have been shown to ameliorate organ and tissue injury not only by acting as antioxidants but also by modulating key signaling pathways involved in inflammation, apoptosis and autophagy (Karwasra et al., 2016; Potocnjak and Domitrovic, 2016). However, the drug–phytochemical interaction that occurs between medicaments and natural phytochemical compounds can modulate the effectiveness of drug treatment in an unpredictable way

* Corresponding author. Department of Medical Chemistry, Biochemistry and Clinical Chemistry, Faculty of Medicine, University of Rijeka, B. Branchetta 20, 51000, Rijeka, Croatia.
E-mail address: robert.domitrovic@medri.uniri.hr (R. Domitrović).

https://doi.org/10.1016/j.fct.2019.110676
Received 12 April 2019; Received in revised form 11 July 2019; Accepted 12 July 2019
Available online 12 July 2019

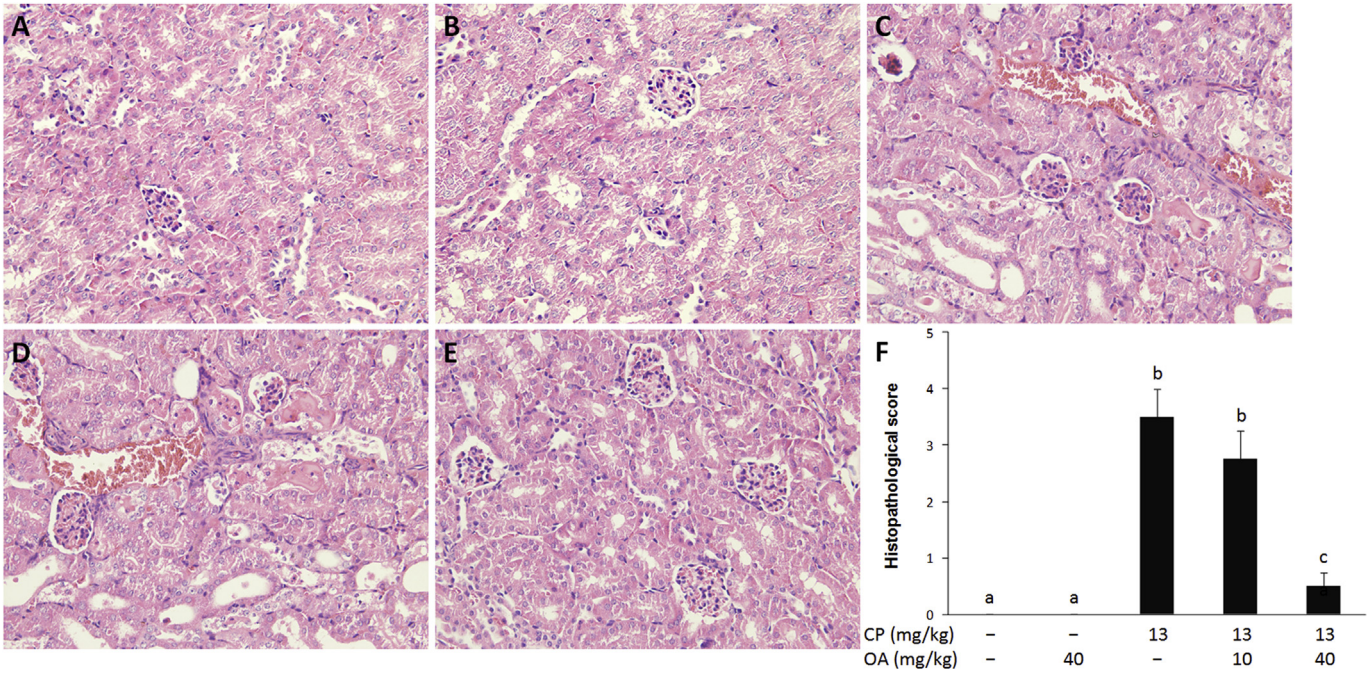

Fig. 1. Hematoxylin and eosin staining showing kidney histopathology. Mice were treated by vehicle (A), oleanolic acid (OA) 40 mg/kg (B), cisplatin (CP) 13 mg/kg (C), CP + OA 10 mg/kg (D) and CP + OA 40 mg/kg (E). CP intoxication resulted in renal tubular necrosis with dilatation of tubules and tubular cast formation. Histopathological changes in renal tissue treated by CP were dose-dependently ameliorated by OA. Histopathological injury score (F). Representative images from at least 10 high power fields (HPF). Original magnification ×400. Each value represents the mean ± SD for 5 mice. Data were analyzed by one-way ANOVA followed by Tukey's post-hoc test. Different letters indicate a statistically significant difference between groups ($P < 0.05$).

Table 1
Body weight change, relative kidney weight and serum markers of kidney damage. Mice were treated with OA by gavage for two days, 48 h after intraperitoneal injection of CP (13 mg/kg). Control and OA only treated mice received vehicle and OA 40 mg/kg, respectively.

	Body weight change (%)	Relative kidney weight	Creatinine (μmol/L)	BUN (mmol/L)
Control	+2.7 ± 0.6^{a}	6.9 ± 0.3^{a}	35.1 ± 1.9^{a}	18.8 ± 2.5^{a}
OA 40 mg/kg	+1.9 ± 1.1^{a}	6.8 ± 0.3^{a}	36.6 ± 2.2^{a}	19.7 ± 2.1^{a}
CP	- 18.3 ± 3.8^{b}	8.9 ± 0.2^{b}	164.7 ± 24.8^{b}	105.5 ± 11.2^{b}
CP + OA 10 mg/kg	- 15.1 ± 3.1^{b}	8.1 ± 0.3^{c}	119.5 ± 14.2^{c}	77.8 ± 8.4^{c}
CP + OA 40 mg/kg	- 5.7 ± 1.8^{d}	7.4 ± 0.4^{a}	40.6 ± 5.1^{a}	21.7 ± 1.7^{a}

Relative kidney weight is expressed as [(kidney weight/body weight)*1000]. Each value represents the mean ± SD for 5 mice. Means within columns sharing the same letter are not significantly different from each other ($P < 0.05$). CP, cisplatin; OA, oleanolic acid; BUN, blood urea nitrogen.

(Potocnjak et al., 2018).

Pentacyclic triterpenes are the class of phytochemicals widespread in different parts of various edible and medicinal plants (Jager et al., 2009). This class of triterpenoids attracted much attention because of their remarkable broad spectrum of pharmacological activities (Salvador et al., 2017). Oleanolic acid (OA) is a natural pentacyclic triterpene compound that possesses antioxidant (Zhang et al., 2018), anti-inflammatory (Kashyap et al., 2016), antidiabetic (Castellano et al., 2013), hepatoprotective (Liu et al., 2019), anticancer (Ziberna et al., 2017), antimicrobial and antiparasitic (Ayeleso et al., 2017) properties. OA exists widely in fruits, vegetables and medicinal herbs, and it has been found in more than 1600 plants (Liu et al., 2019).

We hypothesize that OA could not only protect mice kidneys against CP-induced AKI but also chemosensitize cancer cells to CP. We examined the modulation of oxidative stress, inflammatory response, apoptosis and autophagy, as well as the changes in mitogen activated protein kinase (MAPK), signal transducer and activator of transcription 3 (STAT3) and nuclear factor-kappa B (NF-κB) signaling pathways, involved in the regulation of apoptosis, autophagy and inflammation, in the kidneys of CP-intoxicated mice. In addition, we studied the effect of OA on the modulation of CP cytotoxicity in human cervical cancer cells.

2. Materials and methods

2.1. Chemicals

Oleanolic acid (97%), cisplatin (99.99%), tris(hydroxymethyl)aminomethane (Tris), HEPES (4-(2-hydroxyethyl)-1-piperazineethanesulfonic acid), dimethyl sulfoxide (DMSO) Tween-80, Tween-20, and sodium dodecyl sulfate (SDS) were purchased from Sigma-Aldrich (Steinheim, Germany). Diagnostic kits for blood urea nitrogen (BUN) and serum creatinine were from DiaSys (Holzheim, Germany). Polyvinylidene fluoride (PVDF) membrane, phosphatase inhibitor PhosSTOP and non-fat dry milk were purchased from Roche Diagnostics GmbH (Mannheim, Germany). EnVision + System, Peroxidase/DAB kit with secondary anti-mouse/anti-rabbit antibodies (K500711) were from DAKO Corporation (Carpinteria, CA, USA). Superoxide Dismutase (SOD) Assay Kit was purchased from Cayman Chemical (Ann Arbor, MI, USA). Anesthetic and analgesic (Narketan and Xylapan) were purchased from Vétoquinol (Bern, Switzerland). Antibodies to nuclear factor-kappa B (NF-κB) p65 (ab7970), tumor necrosis factor-alpha (TNF-α, ab1793), 4-hydroxynonenal (4-HNE, ab46545), beta-actin (β-actin, ab8226), heme oxygenase-1 (HO-1, ab13243), superoxide dismutase 2 (SOD2, ab13533), Bcl-2 (ab7973),

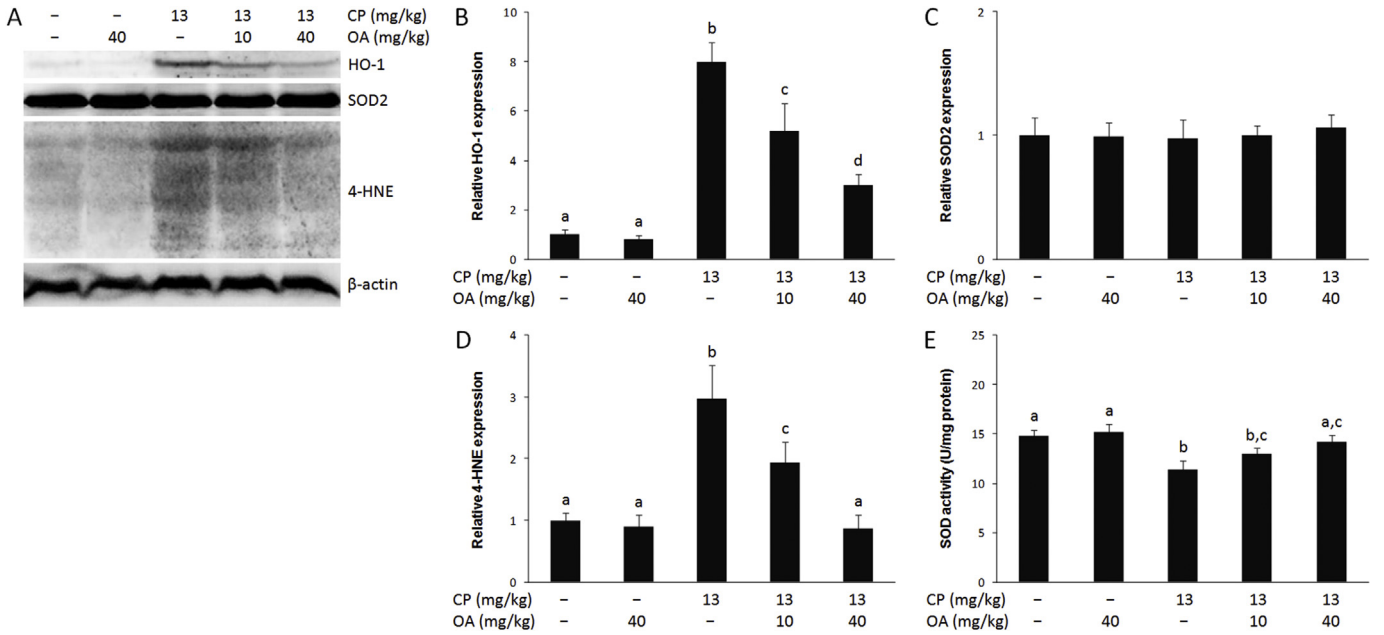

Fig. 2. Representative immunoblots of heme oxygenase-1 (HO-1), superoxide dismutase 2 (SOD2) and 4-hydroxynonenal (4-HNE) expression in kidney lysates (A). Administration of cisplatin (CP) resulted in increased HO-1 (B) and 4-HNE (D) expression, which was decreased by oleanolic acid (OA) treatment in a dose-dependent manner. The expression of SOD2 remained unchanged in all treatments (C). However, the total SOD activity in mice kidney lysates was reduced by CP treatment and restored by OA 40 mg/kg (E). The density of bands was normalized to β-actin. Each value represents the mean ± SD for 5 mice. Data were analyzed by one-way ANOVA followed by Tukey's post-hoc test. Different letters indicate a statistically significant difference between groups ($P < 0.05$).

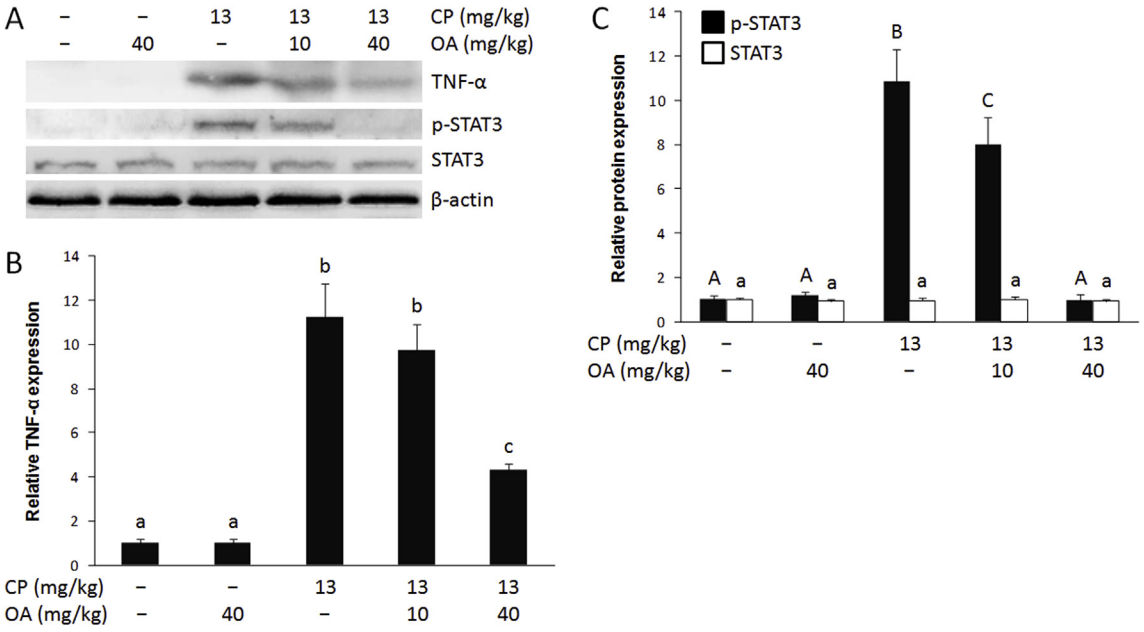

Fig. 3. Representative immunoblots of tumor necrosis factor-alpha (TNF-α), signal transducer and activator of transcription 3 (STAT3) and phosphorylated STAT at Ser727 (p-STAT3) expression in kidney lysates (A). Administration of cisplatin (CP) resulted in an increased TNF-α (B) and p-STAT3 expression while STAT3 expression remained unchanged (C). Treatment with oleanolic acid (OA) decreased TNF-α expression as well as p-STAT3 expression in CP-treated mice. The density of bands was normalized to β-actin. Each value represents the mean ± SD for 5 mice. Data were analyzed by one-way ANOVA followed by Tukey's post-hoc test. Different letters indicate a statistically significant difference between groups ($P < 0.05$).

caspase-9 (ab185719), p21 (ab109199), and microtubule-associated protein 1A/1B-light chain 3 II B (LC3B-I/II, ab48394) were purchased from Abcam (Cambridge, UK). Antibodies to extracellular regulated kinase (ERK) 1/2 (#4695), phosphorylated ERK1/2 (p-ERK, Thr202/Tyr204) (#4370), c-Jun N-terminal kinase (JNK) 1/2/3 (#9251), phosphorylated JNK1/2/3 (p-JNK, Thr183/Tyr185) (#9252), p38 (#8690), phosphorylated p38 (p-p38, Thr180/Tyr182) (#4511), poly (ADP-ribose) polymerase (PARP, #9542), STAT3 (#12640), p-STAT3 (Ser727, #9136), cleaved caspase-3 (#9661), SignalFire Elite ECL reagent and XTT (2,3-bis(2-methoxy-4-nitro-5-sulfophenyl)-2H-tetrazolium-5-carboxanilide inner salt) Cell Viability Kit (#9095) were from Cell Signaling Technologies (Beverly, MA, USA). Antibodies to caspase-3 (sc7272), autophagy-related protein 5 (Atg5, sc133158) and radioimmunoprecipitation assay (RIPA) lysis buffer with protease inhibitors included (2 mM phenylmethyl sulphonyl fluoride, 1 mM sodium orthovanadate and 2 μg/ml of each aprotinin, leupeptin and pepstatin)

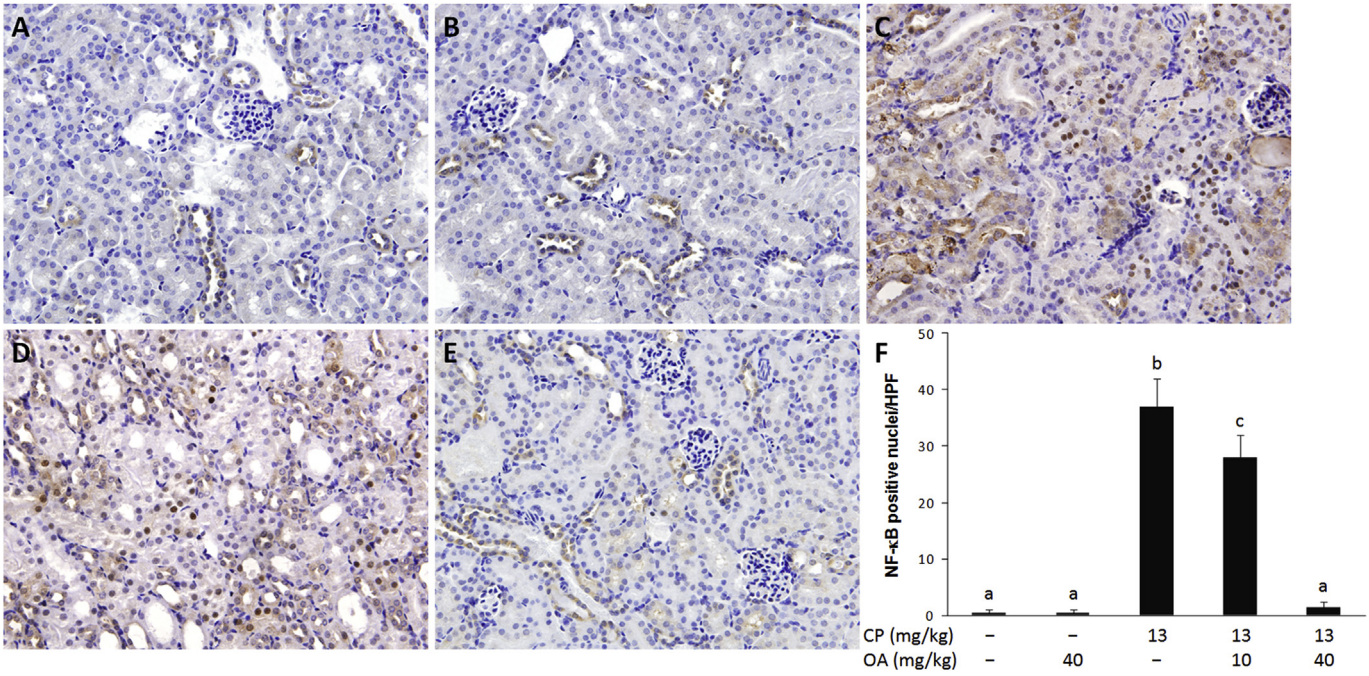

Fig. 4. Immunohistochemistry staining of nuclear factor kappa B (NF-κB) cellular localization in the corticomedullary junction of mice kidneys. Mice were treated by vehicle (A), oleanolic acid (OA) 40 mg/kg (B), cisplatin (CP) 13 mg/kg (C), CP + OA 10 mg/kg (D) and CP + OA 40 mg/kg (E). Arrows show NF-κB immunopositive nuclei. Representative images from at least 10 high power fields (HPF). Original magnification ×400. Measurement of the intensity of NF-κB immunostaining (F). Each value represents the mean ± SD for 5 mice. Different letters indicate a statistically significant difference between groups ($P < 0.05$).

(sc-24948) were from Santa Cruz Biotechnology (Dallas, Texas, USA). Secondary antibodies, horseradish peroxidase (HRP)-conjugated goat polyclonal anti-mouse IgG (ab79023) and HRP-conjugated goat polyclonal anti-rabbit IgG (ab6721) were from Abcam. All other chemicals were of the highest grade commercially available.

2.2. Animals

Male BALB/cN mice from the breeding colony of Faculty of Medicine (LAMRI), Rijeka, Croatia, 12–15 week old, weighing 25–32 g, were maintained in plastic cages at 12 h light/dark cycle, at constant temperature (20 ± 1 °C) and humidity (50 ± 5%). Mice were fed a standard rodent diet (type 4RF21 GLP, Mucedola, Italy) and water *ad libitum*. All experimental procedures were performed according to the appropriate laws and were approved by the Ethical Committee of the Faculty of Medicine, University of Rijeka (HR-POK-024). During the experiment we monitored the animals daily. We checked their behavior and appearance in order to notice the occurrence of pain, suffering or anxiety. All mice tolerated the treatments well.

2.3. In vivo experimental design

Mice were randomly divided into 5 groups with 5 animals per group. Group I received vehicle by oral gavage, group II received OA (40 mg/kg) dissolved in DMSO/water (5% v/v) solution, group III received a single intraperitoneal (i.p.) injection of CP (13 mg/kg) and groups IV and V were orally treated with OA (10 and 40 mg/kg, respectively) for two consecutive days, 48 h after CP administration. Previous studies showed that AKI starts to develop two days after cisplatin administration (Zhang et al., 2014; Pabla et al., 2015). We opted for this time point to investigate the therapeutic activity of OA against developing kidney injury induced by CP rather than its preventive activity (Potocnjak et al., 2016; , 2017). Doses of OA were selected based on preliminary studies. Four days after CP administration, blood was collected from retro-orbital sinus of anesthetized mice (Narketan and Xylapan, i.p. injection, according to the manufacturer's instructions) into microtubes, allowed to clot for one 1 h at room temperature, after which serum was separated and used for biochemical analyses. Mice were euthanized and kidneys were removed. Right kidney of each animal was fixed in phosphate-buffered 4% paraformaldehyde solution for 48 h for histological analysis, while left kidney was frozen at −80 °C and used for western blotting and measurement of enzyme activity.

2.4. Hela cells

The human cervical cancer HeLa cells (obtained from American Type Culture Collection (ATCC), Rockville, MD, USA), were grown in Roswell Park Memorial Institute (RPMI) Medium 1640 supplemented with 10% fetal bovine serum, 2 mM L-glutamine, penicillin 10 000 UI/mL and streptomycin 10 000 mg/mL (all from Lonza, Verviers, Belgium) in tissue culture flasks (TPP, Trasadingen, Switzerland) at 37 °C in a 5% CO_2 humidified atmosphere and harvested by trypsinization in 0.01% ethylenediaminetetraacetic acid (EDTA) (Lonza, Verviers, Belgium).

2.5. In vitro experimental design

Cells were treated with OA (5, 10, 20 and 30 μM), CP (25 μM), combinations of CP and OA and medium only as a control. Before treatments, cells were harvested and counted using Neubauer cell counting chamber (Roth, Karlsruhe, Germany), then transferred to RPMI without antibiotics and 1×10^5 cells per ml were seeded in flasks and flat bottom 96-well chambers (TPP, Trasadingen, Switzerland). Cells were grown until 80% confluence, washed twice in phosphate buffered saline (PBS), pH 7.4, and then exposed to RPMI supplemented with 10% fetal bovine serum, 2 mM L-glutamine, Tween-80 and DMSO containing the desired concentrations of OA and CP for 24 h (the final concentrations of DMSO and Tween-80 in the medium were 0.005% and 0.1%, respectively).

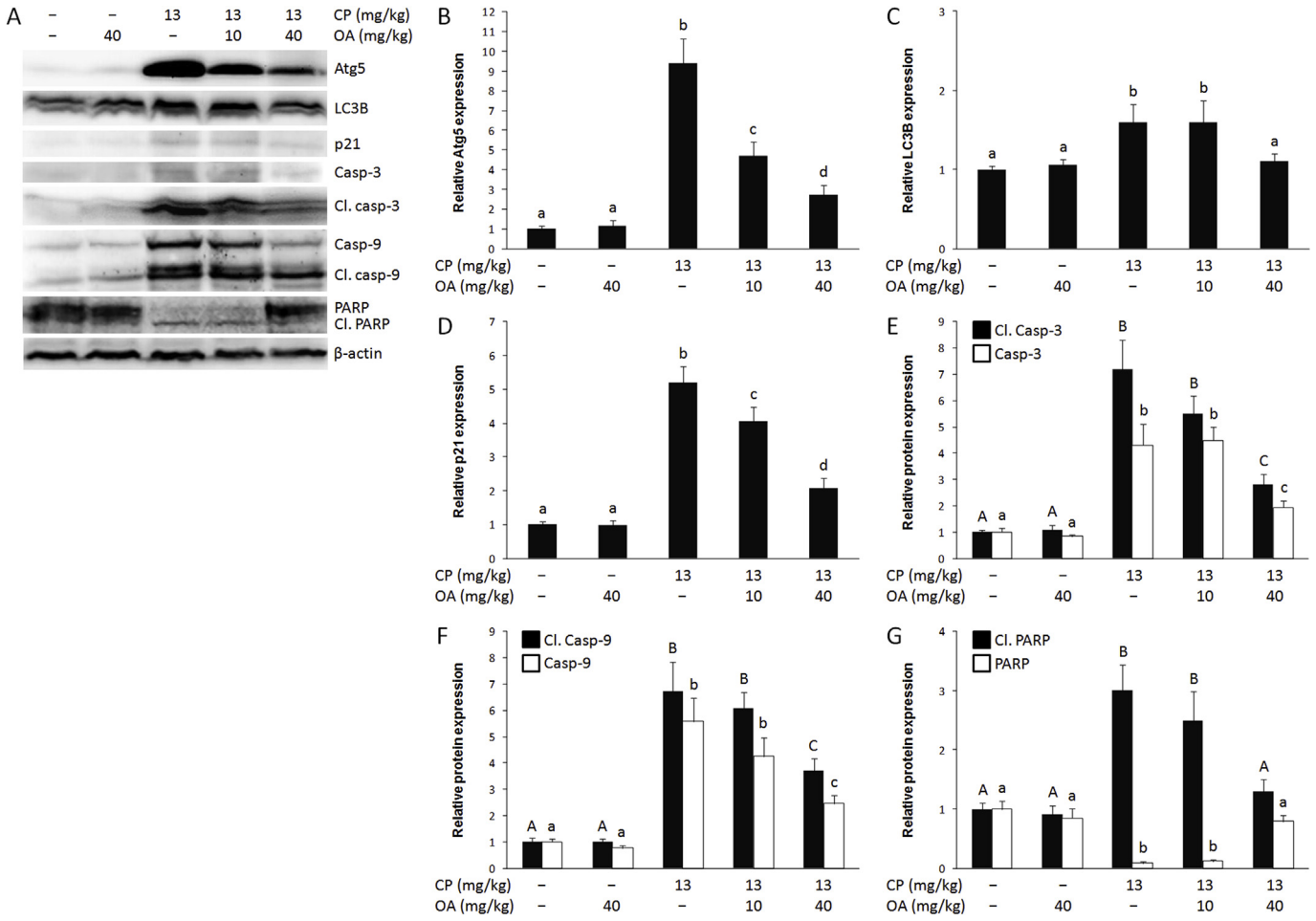

Fig. 5. Representative immunoblots of autophagy-related protein 5 (Atg5), microtubule-associated protein 1 light chain 3B-I/II (LC3B-I/II), p21, caspase-3, caspase-9 and poly (ADP-ribose) polymerase (PARP) expression in mice kidney tissue lysates (A). Cisplatin (CP) treatment increased Atg5 (B) and LC3B-I/II (C) expression which was ameliorated in a dose-dependent manner by oleanolic acid (OA). The increased expression of p21 in CP treatment was decreased by OA (D). OA also decreased CP-induced caspase-3 and cleaved caspase-3 expression (E). Similarly, the expression of caspase-9 (F) and PARP (G) and their cleaved forms was increased by CP treatment but dose-dependently ameliorated by OA. The density of bands was normalized to β-actin. Each value represents the mean ± SD for 5 mice. Data were analyzed by one-way ANOVA followed by Tukey's post-hoc test. Different letters indicate a statistically significant difference between groups ($P < 0.05$).

2.6. Cell viability assay

The XTT assay was used to determine the effect of different treatments on HeLa cell viability. Non-viable cells lose their metabolic capability to reduce XTT into colored formazan dye. After treatments, the prepared reagent was added and the absorbance was measured at 450 nm using a microplate reader (BioTek Elx808, Winooski, VT, USA). Each experiment was performed 3 times in triplicates.

2.7. Serum biochemistry

Blood urea nitrogen (BUN) and serum creatinine were determined colorimetrically (Bio-Tek EL808 Ultra Microplate Reader, BioTek Instruments, Winooski, VT, USA), according to the manufacturer's instructions.

2.8. Histopathology

Paraformaldehyde-fixed kidney tissue was embedded in paraffin, cut into 4 μm thick sections, deparaffinized using standard techniques and stained with hematoxylin and eosin (HE). Evaluation of kidney tissue injury was determined by scoring tubular dilatation, cell necrosis and cast formation by light microscope in at least 10 different fields (×400 original magnification) (Olympus BX51, Tokyo, Japan). The kidney histopathology was scored 0–5; 0 = no damage, 1 = 10% of the corticomedullary junction injured, 2 = 10–25%, 3 = 25–50%, 4 = 50–75%, 5 = more than 75% (Leemans et al., 2005).

2.9. Western blot

Western blot analysis was performed on lysates of mice kidneys and HeLa cells in RIPA buffer with the addition of protease and phosphatase inhibitors. Volume equivalents of 30 or 60 μg of proteins were separated by 8%, 12.5% or gradient SDS-polyacrylamide gel electrophoresis and transferred onto PVDF membrane. The membranes were blocked with 5% non-fat milk in Tris-buffered saline (TBS) containing 0.1% Tween-20 (TBST), 0.01 M, pH 7.4 and incubated for 2 h at room temperature or at 4 °C overnight with primary antibodies against 4-HNE (1:2000), HO-1 (1:2000), SOD2 (1:4000), TNF-α (1:1000), p21 (1:1000), caspase-3 (1:300), cleaved caspase-3 (1:300), caspase-9 (1:1000), PARP (1:1000), Bcl-2 (1:100), Atg5 (1:1000), LC3B-I/II (1:500), ERK1/2 (1:1000), p-ERK1/2 (1:2000), JNK1/2/3 (1:1000), p-JNK1/2 (1:1000), p38 (1:1000), p-p38 (1:1000), STAT3 (1:1000), p-STAT3 Ser727 (1:1000) or β-actin (1:5000). The membranes were washed in TBST and incubated for 1 h at room temperature with secondary antibodies to rabbit IgG (1:80000), mouse IgG (1:50000) or mouse IgGκ (1:3000). After washing in TBST, signals were detected by using SignalFire Elite ECL Reagent and scanned (Allianze 4.0,

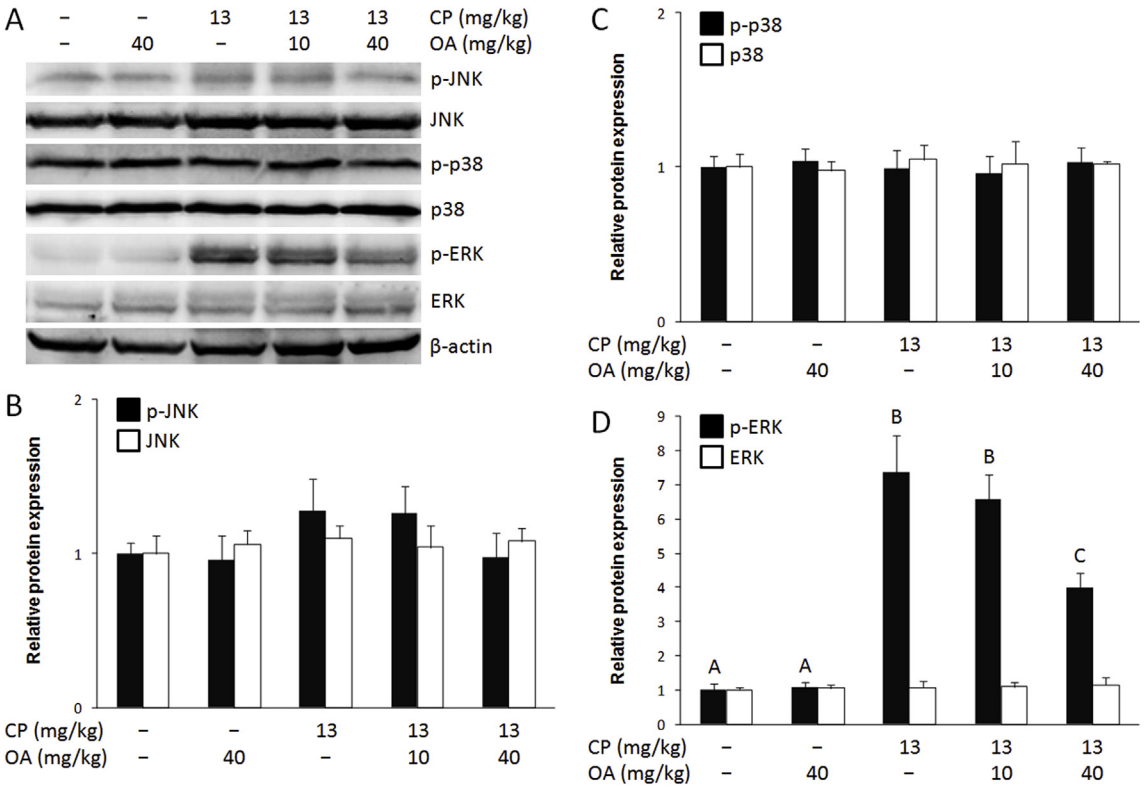

Fig. 6. Representative immunoblots of c-Jun N-terminal kinase 1/2/3 (JNK), phosphorylated JNK1/2 (p-JNK), p38, phosphorylated p38 (p-p38), extracellular regulated kinase 1/2 (ERK1/2) and phosphorylated ERK1/2 (p-ERK) expression in mice kidney lysates (A). The expression of JNK1/p-JNK1 (the 46 kDa subunit) (B) and p38/p-p38 (C) did not change in the experiment. Treatment with cisplatin (CP) resulted in increased expression of p-ERK1/2 compared to controls, which was reduced by oleanolic acid (OA) 40 mg/kg (D). The density of bands was normalized to β-actin. Each value represents the mean ± SD for 5 mice. Data were analyzed by one-way ANOVA followed by Tukey's post-hoc test. Different letters indicate a statistically significant difference between groups ($P < 0.05$).

Cambridge, UK). The intensity of the bands was assayed by computer image analysis software (ImageJ software, NIH, Bethesda, MD, USA).

2.10. SOD activity

The total SOD activity in the kidney, lysed in HEPES buffer, was determined colorimetrically (Bio-Tek EL808 Ultra Microplate Reader, BioTek Instruments, Winooski, VT, USA), according to the manufacturer's instructions.

2.11. Immunohistochemistry

Immunohistochemical analysis was performed on the 4 μm thick paraffin kidney tissue sections, previously deparaffinized and rehydrated, followed by high-temperature antigen retrieval in citrate buffer solution (0.01 M, pH 6.0) for 20 min. Endogenous peroxidase activity was blocked with 3% hydrogen peroxide in methanol for 30 min. The slides were washed with phosphate buffer saline (PBS, pH 7.2) and incubated with 5% bovine serum albumin (BSA) in PBS for 1 h, followed by incubation with primary antibody against NF-kB p65 subunit (1:1000) in 1% BSA in PBS overnight at 4 °C in a humidified chamber. Specific binding of primary antibodies was detected using a DAKO EnVision + System kit according to the manufacturer's instructions. Slices were counterstained with hematoxylin and dehydrated. The immunostaining intensity was analyzed by light microscopy (Olympus BX51, Tokyo, Japan).

2.12. Statistical analysis

Data were analyzed by StatSoft STATISTICA version 13.0 computer software (StatSoft Inc., Tulsa, USA). Comparison of mean values between groups was performed by one-way ANOVA and Tukey's post-hoc test. Values in the text are means ± standard deviation (SD). Means with different letters significantly differ from each other. Differences with $P < 0.05$ were considered statistically significant.

3. Results

3.1. OA attenuates CP-induced kidney injury

Body weight and relative kidney weight of control and OA only treated mice were similar. CP administration resulted in kidney injury (Fig. 1), decreased body weight compared to control mice and mice treated only with OA and increased relative kidney weight (Table 1). The BUN and serum creatinine levels, increased by CP administration, were dose-dependently attenuated by OA (Table 1). The control mice (Fig. 1A) and mice treated with OA (Fig. 1B) had normal kidney architecture. Administration of CP resulted in tubular dilatation, epithelial degeneration, peritubular and glomerular congestion and cast formation (Fig. 1C), increasing the renal injury score from 0 in controls to 3.5 ± 0.5. Treatment of CP-intoxicated mice by OA (Fig. 1D and E) notably attenuated kidney injury in a dose-dependent manner, resulting in the decreased histopathological score (2.8 ± 0.5 and 0.5 ± 0.25, respectively) compared to CP-treated mice.

3.2. OA attenuates CP-induced oxidative stress in the kidneys

Western blot analysis (Fig. 2A) showed that CP administration was associated with an increased expression of oxidative stress markers HO-1 and 4-HNE in kidneys compared to control mice and mice treated with OA only (Fig. 2B and C). Treatment of CP-intoxicated mice with OA dose-dependently decreased expression of both enzymatic (HO-1)

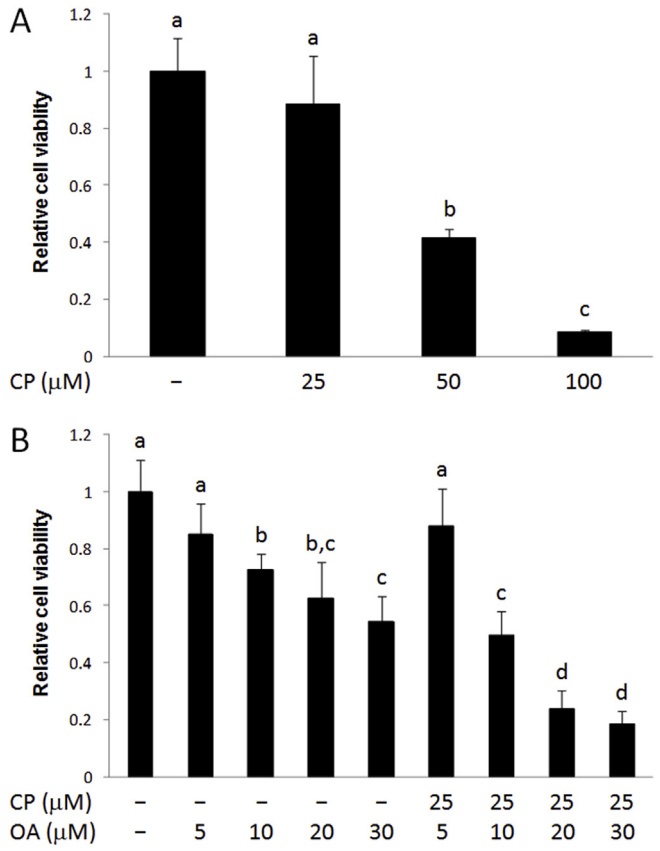

Fig. 7. The dose-dependent effect of OA and CP on HeLa cells viability. The cells were treated with OA, CP and their combination for 24 h and cell viability were measured by the 2,3-bis(2-methoxy-4-nitro-5-sulfophenyl)-2H-tetrazolium-5-carboxanilide inner salt (XTT) assay. The percentage of cytotoxicity was calculated in comparison to untreated cells taken as 100%. Values are expressed as mean ± SD from three independent experiments. Data were analyzed by one-way ANOVA followed by Tukey's post-hoc test. Different letters indicate a statistically significant difference between groups ($P < 0.05$). The 50% inhibitory concentration (IC_{50}) was determined using the non-linear regression analysis.

and non-enzymatic (4-HNE) oxidative stress markers. On the other hand, there were no statistically significant differences in kidney expression of SOD2 with or without treatment with OA in CP-induced kidney injury (Fig. 2D). Therefore, we measured the SOD activity in the kidney lysates (Fig. 2E). The SOD activity was reduced in CP-treated mice compared to control and OA only treated groups, whereas treatment with OA 40 mg/kg prevented the loss of SOD activity.

3.3. OA suppresses CP-induced renal inflammation

CP administration increased renal expression of TNF-α (Fig. 3A) compared to control and OA only treated groups. A lower dose of OA (10 mg/kg) did not cause changes in TNF-α expression, however, a higher dose of OA (40 mg/kg) decreased TNF-α expression (Fig. 3B). The immunohistochemical evaluation showed more intense expression of NF-κB p65 subunit in kidneys of CP-treated mice (Fig. 4C) compared to controls (Fig. 4A and B) or OA-treated mice (Fig. 4D and E). Overexpression of NF-κB p65 was noticed both in the cytoplasm and the nuclei of tubular cells. A lower dose of OA reduced nuclear NF-κB p65 immunopositivity, which diminished by a higher dose of OA (40 mg/kg), with concomitant reduction of the cytoplasmic staining intensity. OA dose-dependently attenuated an elevated p-STAT3 expression in the kidneys of CP-intoxicated mice (Fig. 3C).

3.4. OA suppresses CP-induced autophagy in the kidneys

Western blot analysis (Fig. 5A) showed an increased expression of Atg5 and LC3B-I/II in CP-treated mice compared to control and OA only treated mice and indicated the induction of autophagy in mice kidneys. Treatment of CP-intoxicated mice with OA dose-dependently reduced renal expression of Atg5 (Fig. 5B). The expression of LC3B-I/II was decreased only with a higher dose of OA (40 mg/kg).

3.5. OA attenuates CP-induced apoptosis and inhibition of cell cycle in the kidneys

CP-intoxication resulted in increased p21 expression in mice kidneys, which was reduced by a higher dose of OA (40 mg/kg) (Fig. 5D). In addition, treatment with CP resulted in an increased cleavage of caspase-3, caspase-9 and PARP in the kidneys compared to control mice and mice treated only with OA (Fig. 5E, F and 5G). A lower dose of OA (10 mg/kg) did not cause changes in the expression of apoptotic proteins, but a higher dose (40 mg/kg) resulted in their reduced expression.

3.6. OA attenuated CP-induced renal activation of ERK1/2

CP increased renal expression of p-ERK1/2 compared to control and OA only treated mice (Fig. 6A and D), whereas the expression of other MAPKs remained unchanged (Fig. 6B and C). A lower dose (10 mg/kg) of OA did not cause changes in the ERK expression, but a higher dose (40 mg/kg) resulted in reduced expression of ERK.

3.7. OA decreases the viability of HeLa cells

OA exhibited a dose-dependent inhibition of HeLa cell viability, with IC_{50} = 39 μM (Fig. 7B) Interestingly, the lowest dose of OA (5 μM) did not modulate the viability of HeLa cells treated with CP, however, higher doses of OA (10, 20 and 30 μM) induced the apparent synergism with CP in reducing the cell viability, resulting in lower IC_{50} (10 μM). The dose of CP (25 μM) used in the current study had a minimal effect on the HeLa cell viability (Fig. 7A).

3.8. OA chemosensitizes HeLa cells to CP-induced autophagy

Western blot analysis of HeLa cells lysates (Fig. 8A) showed that OA induced cleavage of caspase-3 (Fig. 8B) and PARP (Fig. 8C). Concomitantly, the highest dose of OA (30 μM) increased LC3B-II expression (Fig. 8E), which was accompanied by reduced expression of Bcl-2 (Fig. 8D). Treatment of the cells with CP resulted in a marked increase in caspase-3 and PARP cleavage, with a concomitant increase in LC3B-II expression and reduction of Bcl-2 expression. Interestingly, co-treatment with CP and OA dose-dependently suppressed PARP and caspase-3 cleavage, with concomitant suppression of Bcl-2 expression and increased LC3B-II expression.

4. Discussion

In the current study, CP treatment induced oxidative injury in mice kidneys, which was evidenced by an increased expression of antioxidant and cytoprotective enzyme HO-1 and the final product of lipid peroxidation, 4-HNE. Renal oxidative stress was dose-dependently ameliorated by OA, suggesting its ROS scavenging activity in CP-induced kidney injury. The expression of SOD2 did not change under the experimental conditions, however, the activity of SOD was decreased by CP treatment and was restored by OA. The blockage of ROS production from the superoxide radical sources, such as xanthine oxidase, NADPH oxidase and mitochondrial respiratory complexes, has been previously shown to alleviate AKI in experimental models (Dennis and Witting, 2017).

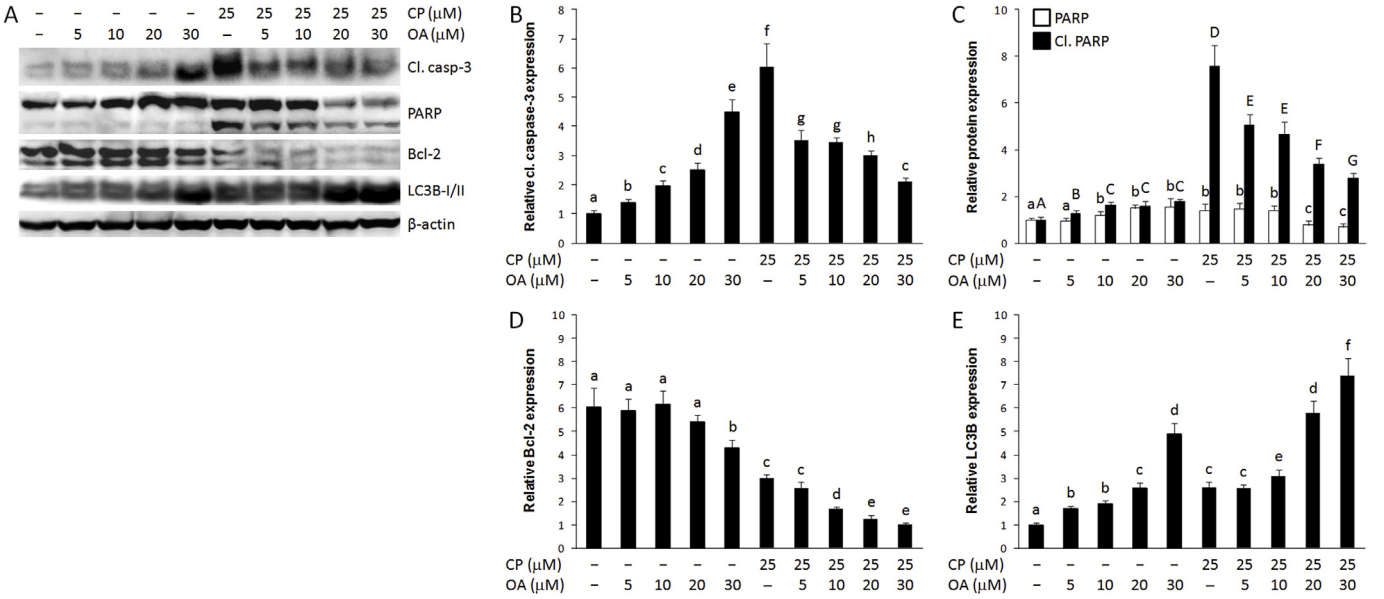

Fig. 8. Representative immunoblots of cleaved caspase-3, poly (ADP-ribose) polymerase (PARP), Bcl-2 and microtubule-associated protein 1 light chain 3B-I/II (LC3B-I/II) expression in HeLa cell lysates (A). Oleanolic acid (OA) increased expression of cleaved caspase-3 (B) and PARP (C). Concomitantly, the expression of Bcl-2 (D) decreased and LC3B-II (E) increased. Cisplatin (CP) treatment induced a marked increase in caspase-3 and PARP cleavage, with reduced Bcl-2 and increased LC3B-II expression compared to controls. OA dose-dependently reduced cleavage of caspase-3 and PARP and Bcl-2 expression with concomitant induction of LC3B-II compared to CP treatment. The density of bands was normalized to β-actin. Each value represents the mean ± SD from three independent experiments. Data were analyzed by one-way ANOVA followed by Tukey's post-hoc test. Different letters indicate a statistically significant difference between groups ($P < 0.05$).

In response to renal injury, various inflammatory proteins such as cytokines are produced (Perse and Veceric-Haler, 2018). The production of TNF-α after CP administration seems to be NF-κB dependent and acts on endothelial adhesion molecules to attract inflammatory cells (Pabla and Dong, 2008). In the current study, administration of OA reduced CP-induced NF-κB p65 nuclear translocation, observed as the reduced number of NF-κB immunopositive nuclei in proximal tubular cells, as well as the expression of TNF-α. These findings suggest the anti-inflammatory effect of OA, which is in the agreement with our previous results (Potocnjak et al., 2017; Potocnjak and Domitrovic, 2016). The ability of OA to attenuate the induction of NF-κB suggests its potential as an anti-inflammatory agent in CP-induced kidney injury.

STAT proteins are a family of transcription factors that are activated by direct tyrosine phosphorylation, which then translocate to the nucleus (Shuai, 1994). Cytokines, including TNF-α, have been found to induce pro-inflammatory signaling through activation of STAT3 (Mori et al., 2011) and modulate inflammatory response through the ERK pathway (Wang et al., 2013). In agreement with the pro-inflammatory role of STAT3 in AKI (Mori et al., 2011; Potocnjak et al., 2017), our results showed increased STAT3 phosphorylation after CP intoxication in mice. However, treatment with OA markedly suppressed STAT3 activation, supporting the anti-inflammatory role of OA in CP-induced AKI.

The cyclin-dependent kinase inhibitor p21, in the kidney is upregulated after CP treatment and plays a protective role against its toxicity (Price et al., 2004). p21 plays multiple roles in the DNA damage response, including regulation of cell cycle, apoptosis and gene transcription (Cazzalini et al., 2010). Previously, it was shown that CP-induced hydroxyl radical formation causes single-strand DNA breakage followed by activation of PARP to repair the damaged DNA and induces apoptotic events that are mediated by ROS (Chirino and Pedraza-Chaverri, 2009). Likewise, in the current study, CP intoxication resulted in activation of caspase-3 and caspase-9 as well as PARP cleavage, suggesting induction of renal tubular cell apoptosis. Concomitantly, a block of cell cycle progression was indicated by an increase in p21 expression. CP-induced apoptosis and inhibition of cell cycle were attenuated by OA, suggesting the anti-apoptotic effect of OA, which can be attributed to its antioxidant activity.

Autophagy occurs in AKI as an important protective mechanism for cell survival and protects kidney proximal tubules against AKI by eliminating ROS producing mitochondria during CP treatment (Periyasamy-Thandavan et al., 2008; Takahashi et al., 2012). Atg5 is a critical protein required for autophagy at the stage of autophagosome-precursor synthesis and its deletion in yeast or mammalian cells/mice effectively blocks autophagy (Kuma et al., 2004). Atg5 initiates the formation of the autophagosome membrane and the fusion of autophagosomes and lysosomes, and it is also involved in both intrinsic and extrinsic apoptosis (Ye et al., 2018). The Atg12–Atg5 protein conjugate is essential for autophagosome formation. It localizes to autophagosome precursors and dissociates just before or after completion of autophagic-vacuole formation (Mizushima et al., 2001). Microtubule-associated protein 1 light chain 3B (LC3B) is required for completion of autophagosome formation and LC3B-II is specifically targeted to the Atg12–Atg5-associated, elongated autophagosome precursors (Kirisako et al., 1999). In the current study, CP administration increased expression of Atg5 and LC3B-II but OA administration dose-dependently decreased the expression of both proteins. These findings indicate the anti-autophagic effect of OA, which could be attributed to its antioxidant properties (Takahashi et al., 2012).

ERK plays a crucial role in CP-induced kidney injury and the inhibition of ERK activation attenuates CP-mediated apoptosis in kidneys (Potocnjak et al., 2016). CP-induced ERK activation precedes p53-mediated DNA damage response as ERK directly phosphorylates p53, resulting in up-regulated expression of p21 and may result in cell cycle arrest and apoptosis promotion (Wang et al., 2000). CP administration increased renal expression of p-ERK1/2 but not JNK and p38. ERK activation was associated with cell cycle inhibition and induction of apoptosis, evidenced by the activation of p21 and cleavage of caspase-3 and -9. Administration of a higher dose of OA to CP-intoxicated mice reduced ERK1/2 phosphorylation, which coincided with the restoration of expression of p21 as well as caspase-3 and -9, suggesting the recovery of cell cycle and the suppression of apoptosis. Since ERK also mediates CP-induced renal inflammation (Jo et al., 2005; Potocnjak et al., 2016), treatment with OA coincided with the reduction of both phospho-NF-κB

and TNF-α expression mice kidneys.

In addition to the renoprotective activity, our *in vitro* study showed that OA chemosensitized HeLa cells to CP cytotoxicity. In doses 5–30 μM, OA showed a modest reduction of the HeLa cell viability, accompanied by the induction of autophagy and apoptosis, which is in agreement with the anticancer properties of OA (Shanmugam et al., 2014). Interestingly, CP-OA co-treatment markedly decreased HeLa cell viability and induced autophagy compared to OA only treatment, with a concomitant block of apoptosis. Although autophagy is recognized as a cell survival process that promotes tumor development, it is also utilized as a caspase-independent form of programmed cell death (Lin end Baehrecke, 2015). Bcl-2 has been recognized as a negative regulator of both apoptosis (Thomadaki and Scorilas, 2006) and autophagy (Pattingre et al., 2005). When apoptosis is blocked, various apoptotic stimuli activate autophagy, resulting in the induction of autophagic cell death (Shimizu, 2015). Reduced expression of Bcl-2 by CP-OA co-treatment in the current study, coincided with the suppression of caspase-3 and PARP cleavage and the induction of LC3B-II expression. This suggests an important role of Bcl-2 in the activation of autophagy as a death mechanism in HeLa cells co-treated with CP and OA. OA has been previously shown to induce autophagic cell death in hepatocellular carcinoma cells (Shi et al., 2016). Various cancer therapeutic agents, including natural compound resveratrol, were shown to directly execute cell death independent of apoptotic machinery (Tan and Shen, 2014).

Taken together, the results of our study show that OA could be considered as the renoprotective natural compound in CP-induced kidney injury. OA is a potential co-treatment in CP-induced AKI according to its antioxidant, anti-inflammatory, anti-apoptotic and anti-autophagic properties that coincided with the regulation of the ERK1/2, STAT3 and NF-κB signaling pathways. Moreover, OA should be considered as a potent CP chemosensitizer of cervical cancer through induction of cytotoxic autophagy. Further studies are required to confirm the beneficial effects of OA in cancer patients undergoing CP chemotherapy, including the adjustment of CP dosage.

Conflicts of interest

The authors declare that there are no conflicts of interest.

Acknowledgements

This research was supported by grants from the University of Rijeka, Croatia (Project uniri-biomed-18-30).

References

Al-Kahtani, M.A., Abdel-Moneim, A.M., Elmenshawy, O.M., El-Kersh, M.A., 2014. Hemin attenuates cisplatin-induced acute renal injury in male rats. Oxid. Med. Cell. Longev 2014, 476430.

Ayeleso, T.B., Matumba, M.G., Mukwevho, E., 2017. Oleanolic acid and its derivatives: biological activities and therapeutic potential in chronic diseases. Molecules 22, 1915.

Castellano, J.M., Guinda, A., Delgado, T., Rada, M., Cayuela, J.A., 2013. Biochemical basis of the antidiabetic activity of oleanolic acid and related pentacyclic triterpenes. Diabetes 62, 1791–1799.

Cazzalini, O., Scovassi, A.I., Savio, M., Stivala, L.A., Prosperi, E., 2010. Multiple roles of the cell cycle inhibitor p21^{CDKN1A} in the DNA damage response. Mutat. Res.-Rev. Mutat. 704, 12–20.

Chirino, Y.I., Pedraza-Chaverri, J., 2009. Role of oxidative and nitrosative stress in cisplatin-induced nephrotoxicity. Exp. Toxicol. Pathol. 61, 223–242.

Cragg, G.M., Newman, D.J., 2013. Natural products: a continuing source of novel drug leads. Biochim. Biophys. Acta 1830, 3670–3695.

Dasari, S., Tchounwou, P.B., 2014. Cisplatin in cancer therapy: molecular mechanisms of action. Eur. J. Pharmacol. 740, 364–378.

Dennis, J.M., Witting, P.K., 2017. Protective role for antioxidants in acute kidney disease. Nutrients 9, E718.

Domitrovic, R., Potocnjak, I., 2016. A comprehensive overview of hepatoprotective natural compounds: mechanism of action and clinical perspectives. Arch. Toxicol. 90, 39–79.

Gomez-Sierra, T., Eugenio-Perez, D., Sanchez-Chinchillas, A., Pedraza-Chaverri, J., 2018. Role of food-derived antioxidants against cisplatin induced-nephrotoxicity. Food Chem. Toxicol. 120, 230–242.

Jager, S., Trojan, H., Kopp, T., Laszczyk, M.N., Scheffler, A., 2009. Pentacyclic triterpene distribution in various plants - rich sources for a new group of multi-potent plant extracts. Molecules 14, 2016–2031.

Jo, S.K., Cho, W.Y., Sung, S.A., Kim, H.K., Won, N.H., 2005. MEK inhibitor, U0126, attenuates cisplatin-induced renal injury by decreasing inflammation and apoptosis. Kidney Int. 67, 458–466.

Karwasra, R., Kalra, P., Gupta, Y.K., Saini, D., Kumar, A., Singh, S., 2016. Antioxidant and anti-inflammatory potential of pomegranate rind extract to ameliorate cisplatin-induced acute kidney injury. Food. Funct. 7, 3091–3101.

Kashyap, D., Sharma, A., Tuli, H.S., Punia, S., Sharma, A.K., 2016. Ursolic acid and oleanolic acid: pentacyclic terpenoids with promising anti-inflammatory activities. Recent Pat. Inflamm. Allergy Drug Discov. 10, 21–33.

Kirisako, T., Baba, M., Ishihara, N., Miyazawa, K., Ohsumi, M., Yoshimori, T., Noda, T., Ohsumi, Y., 1999. Formation process of autophagosome is traced with Apg8/Aut7p in yeast. J. Cell Biol. 147, 435–446.

Kuma, A., Hatano, M., Matsui, M., Yamamoto, A., Nakaya, H., Yoshimori, T., Ohsumi, Y., Tokuhisa, T., Mizushima, N., 2004. The role of autophagy during the early neonatal starvation period. Nature 432, 1032–1036.

Leemans, J.C., Stokman, G., Claessen, N., Rouschop, K.M., Teske, G.J., Kirschning, C.J., Akira, S., van der Poll, T., Weening, J.J., Florquin, S., 2005. Renal-associated TLR2 mediates ischemia/reperfusion injury in the kidney. J. Clin. Investig. 115, 2894–2903.

Lin, L., Baehrecke, E., 2015. Autophagy, cell death, and cancer. Mol. Cell. Oncol. 2, e985913.

Liu, J., Lu, Y.F., Wu, Q., Xu, S.F., Shi, F.G., Klaassen, C.D., 2019. Oleanolic acid reprograms the liver to protect against hepatotoxicants, but is hepatotoxic at high doses. Liver Int. 39, 427–439.

Marullo, R., Werner, E., Degtyareva, N., Moore, B., Altavilla, G., Ramalingam, S.S., Doetsch, P.W., 2013. Cisplatin induces a mitochondrial-ROS response that contributes to cytotoxicity depending on mitochondrial redox status and bioenergetic functions. PLoS One 8, e81162.

Mizushima, N., Yamamoto, A., Hatano, M., Kobayashi, Y., Kabeya, Y., Suzuki, K., Tokuhisa, T., Ohsumi, Y., Yoshimori, T., 2001. Dissection of autophagosome formation using Apg5-deficient mouse embryonic stem cells. J. Cell Biol. 152, 657–667.

Mori, T., Miyamoto, T., Yoshida, H., Asakawa, M., Kawasumi, M., Kobayashi, T., Morioka, H., Chiba, K., Toyama, Y., Yoshimura, A., 2011. IL-1β and TNFα-initiated IL-6-STAT3 pathway is critical in mediating inflammatory cytokines and RANKL expression in inflammatory arthritis. Int. Immunol. 23, 701–712.

Oun, R., Moussa, Y.E., Wheate, N.J., 2018. The side effects of platinum-based chemotherapy drugs: a review for chemists. Dalton Trans. 47, 6645–6653.

Ozkok, A., Edelstein, C.L., 2014. Pathophysiology of cisplatin-induced acute kidney injury. BioMed Res. Int. 2014, 967826.

Pabla, N., Dong, Z., 2008. Cisplatin nephrotoxicity: mechanisms and renoprotective strategies. Kidney Int. 73, 994–1007.

Pattingre, S., Tassa, A., Qu, X., Garuti, R., Liang, X.H., Mizushima, N., Packer, M., Schneider, M.D., Levine, B., 2005. Bcl-2 antiapoptotic proteins inhibit Beclin 1-dependent autophagy. Cell 122, 927–939.

Periyasamy-Thandavan, S., Jiang, M., Wei, Q.Q., Smith, R., Yin, X.M., Dong, Z., 2008. Autophagy is cytoprotective during cisplatin injury of renal proximal tubular cells. Kidney Int. 74, 631–640.

Perse, M., Veceric-Haler, Z., 2018. Cisplatin-induced rodent model of kidney injury: characteristics and challenges. BioMed Res. Int. 2018, 1462802.

Potocnjak, I., Gobin, I., Domitrovic, R., 2018. Carvacrol induces cytotoxicity in human cervical cancer cells but causes cisplatin resistance: involvement of MEK-ERK activation. Phytother Res. 32, 1090–1097.

Potocnjak, I., Broznic, D., Kindl, M., Kropek, M., Vladimir-Knezevic, S., Domitrovic, R., 2017. Stevia and stevioside protect against cisplatin nephrotoxicity through inhibition of ERK1/2, STAT3 and NF-κB activation. Food Chem. Toxicol. 107, 215–225.

Potocnjak, I., Domitrovic, R., 2016. Carvacrol attenuates acute kidney injury induced by cisplatin through suppression of ERK and PI3K/Akt activation. Food Chem. Toxicol. 98, 251–261.

Potocnjak, I., Skoda, M., Pernjak-Pugel, E., Persic, M.P., Domitrovic, R., 2016. Oral administration of oleuropein attenuates cisplatin-induced acute renal injury in mice through inhibition of ERK signaling. Mol. Nutr. Food Res. 60, 530–541.

Pabla, N., Gibson, A.A., Buege, M., Ong, S.S., Li, L., Hu, S., Du, G., Sprowl, J.A., Vasilyeva, A., Janke, L.J., Schlatter, E., Chen, T., Ciarimboli, G., Sparreboom, A., 2015. Mitigation of acute kidney injury by cell-cycle inhibitors that suppress both CDK4/6 and OCT2 functions. Proc. Natl. Acad. Sci. U. S. A. 112, 5231–5236.

Price, P.M., Safirstein, R.L., Megyesi, J., 2004. Protection of renal cells from cisplatin toxicity by cell cycle inhibitors. Am. J. Physiol.-Renal 286, F378–F384.

Salvador, J.A.R., Leal, A.S., Valdeira, A.S., Goncalves, B.M.F., Alho, D.P.S., Figueiredo, S.A.C., Silvestre, S.M., Mendes, V.I.S., 2017. Oleanane-, ursane- and quinonemethide friedelane-type triterpenoid derivatives: recent advances in cancer treatment. Eur. J. Med. Chem. 142, 95–130.

Shanmugam, M.K., Dai, X., Kumar, A.P., Tan, B.K., Sethi, G., Bishayee, A., 2014. Oleanolic acid and its synthetic derivatives for the prevention and therapy of cancer: preclinical and clinical evidence. Cancer Lett. 346, 206–216.

Shi, Y., Song, Q., Hu, D., Zhuang, X., Yu, S., Teng, D., 2016. Oleanolic acid induced autophagic cell death in hepatocellular carcinoma cells via PI3K/Akt/mTOR and ROS-dependent pathway. KOREAN J. PHYSIOL. PHARMACOL. 20, 237–243.

Shimizu, S., 2015. Autophagic cell death and cancer chemotherapeutics. In: Nakao, K., Minato, N., Uemoto, S. (Eds.), Innovative Medicine: Basic Research and Development [Internet]. Springer, Tokyo, pp. 219–226.

Shuai, K., 1994. Interferon-activated signal-transduction to the nucleus. Curr. Opin. Cell

Biol. 6, 253–259.
Takahashi, A., Kimura, T., Takabatake, Y., Namba, T., Kaimori, J., Kitamura, H., Matsui, I., Niimura, F., Matsusaka, T., Fujita, N., Yoshimori, T., Isaka, Y., Rakugi, H., 2012. Autophagy guards against cisplatin-induced acute kidney injury. Am. J. Pathol. 180, 517–525.
Tan, S.H., Shen, H.M., 2014. Autophagic cell death: a real killer, an accomplice, or an innocent bystander? In: Shen, H.M., Vandenabeele, P. (Eds.), Cell Death in Biology and Diseases. Humana Press, New York, pp. 211–232.
Thomadaki, H., Scorilas, A., 2006. BCL2 family of apoptosis-related genes: functions and clinical implications in cancer. Crit. Rev. Clin. Lab. Sci. 43, 1–67.
Wang, S., Wei, Q., Dong, G., Dong, Z., 2013. ERK-mediated suppression of cilia in cisplatininduced tubular cell apoptosis and acute kidney injury. Biochim. Biophys. Acta 1832, 1582–1590.
Wang, X., Martindale, J.L., Holbrook, N.J., 2000. Requirement for ERK activation in cisplatin-induced apoptosis. J. Biol. Chem. 275, 39435–39443.
Ye, X., Zhou, X.J., Zhang, H., 2018. Exploring the role of autophagy-related gene 5 (ATG5) yields important insights into autophagy in autoimmune/autoinflammatory diseases. Front. Immunol. 9, 2334.
Zhang, W., Feng, J., Cheng, B., Lu, Q., Chen, X., 2018. Oleanolic acid protects against oxidative stressinduced human umbilical vein endothelial cell injury by activating AKT/eNOS signaling. Mol. Med. Rep. 18, 3641–3648.
Zhang, D., Liu, Y., Wei, Q., Huo, Y., Liu, K., Liu, F., Dong, Z., 2014. Tubular p53 regulates multiple genes to mediate AKI. J. Am. Soc. Nephrol. 25, 2278–2289.
Ziberna, L., Samec, D., Mocan, A., Nabavi, S.F., Bishayee, A., Farooqi, A.A., Sureda, A., Nabavi, S.M., 2017. Oleanolic acid alters multiple cell signaling pathways: implication in cancer prevention and therapy. Int. J. Mol. Sci. 18.